Development 134, 979-988 (2007) doi:10.1242/dev.02782

Amotl2 is essential for cell movements in zebrafish embryo and regulates c-Src translocation

Huizhe Huang[1,*], Fu-I Lu[2,*], Shunji Jia[1,*], Shu Meng[1], Ying Cao[1], Yeqi Wang[1], Weiping Ma[3], Kun Yin[1], Zilong Wen[3], Jingrong Peng[3], Christine Thisse[2], Bernard Thisse[2,†] and Anming Meng[1,†]

Angiomotin (Amot), the founding member of the Motin family, is involved in angiogenesis by regulating endothelial cell motility, and is required for visceral endoderm movement in mice. However, little is known about biological functions of the other two members of the Motin family, Angiomotin-like1 (Amotl1) and Angiomotin-like2 (Amotl2). Here, we have identified zebrafish amotl2 as an Fgf-responsive gene. Zebrafish amotl2 is expressed maternally and in restricted cell types zygotically. Knockdown of *amotl2* expression delays epiboly and impairs convergence and extension movement, and amotl2-deficient cells in mosaic embryos fail to migrate properly. This coincides with loss of membrane protrusions and disorder of F-actin. Amotl2 partially co-localizes with RhoB- or EEA1-positive endosomes and the non-receptor tyrosine kinase c-Src. We further demonstrate that Amotl2 interacts preferentially with and facilitates outward translocation of the phosphorylated c-Src, which may in turn regulate the membrane architecture. These data provide the first evidence that amotl2 is essential for cell movements in vertebrate embryos.

KEY WORDS: Zebrafish, Epiboly, Convergent extension, c-Src, Angiomotin-like2

INTRODUCTION

The establishment of body plan of vertebrate embryos involves cell proliferation, differentiation and cell migration. In late zebrafish blastula, blastodermal cells start to move in several ways, including: epiboly, through which cells move vegetally around the yolk; involution, which generates the three germ layers; convergence, through which ventral and lateral cells move dorsolaterally; and extension, which results in the elongation of the anteroposterior axis (Solnica-Krezel, 2005; Warga and Kimmel, 1990). Several major signaling pathways, including Fgf, Bmp, Nodal and Wnt, have been found to play important roles in movement of embryonic cells during gastrulation (Ip and Gridley, 2002; Myers et al., 2002; Schier and Talbot, 2005; Thisse and Thisse, 2005), although they are well known to be involved in early patterning (Schier and Talbot, 2005; Thisse and Thisse, 2005; Tian and Meng, 2006). However, only a few downstream effectors involving embryonic cell migration have been identified.

In an effort to screen for factors regulated by Fgf signaling in the zebrafish embryo, we identified using the cDNA microarray technology Amotl2, which belongs to the Motin protein family (Bratt et al., 2002). Amot, the founding member of the Motin family, is characterized as a binding partner of angiostatin, which is an angiogenesis inhibitor (Troyanovsky et al., 2001). In vitro experiments indicate that Amot promotes migration and tube formation of endothelial cells (Troyanovsky et al., 2001). Interestingly, *AMOT* is involved in invasion of tumor cells by promoting angiogenesis (Levchenko et al., 2004), and higher levels of *AMOT* transcripts are detected in human breast tumor tissues (Jiang et al., 2006). The expression of *Amot* is restricted to angiogenic vessels of lobular mammary carcinoma developed in *Her-2/neu* transgenic mice, and thus *Amot* can serve as a target for anti-angiogenic therapy (Holmgren et al., 2006). Mouse *Amot* is expressed in visceral endoderm around gastrulation. *Amot* knockout mice die soon after gastrulation due to improper migration of visceral endoderm (Shimono and Behringer, 2003). Apart from controlling cell motility, Amot may also play a role in regulating the assembly and maintenance of cell-cell junctions (Bratt et al., 2005; Wells et al., 2006). Amotl1 and Amotl2, the other two members of the Motin family, have been previously identified in mammals (Bratt et al., 2002); however, their biological functions in embryonic development have not been reported.

In this study, we demonstrate that *amotl2* is expressed maternally and in a restricted manner as soon as the zygotic genome begins to be expressed. Inhibition of *amotl2* expression by antisense morpholinos causes epiboly arrest and aberrant convergent extension in zebrafish embryos, which coincides with disruption of juxtamembrane actin fibers and formation of membrane protrusion. In vitro analyses reveal that Amotl2 regulates cell migration by binding to and promoting peripheral membrane translocation of the nonreceptor tyrosine kinase c-Src. Taken together, our findings suggest that *amotl2* is essential for cell movement in vertebrate embryos, which might be associated with c-Src translocation.

MATERIALS AND METHODS

Fish strains

Wild-type embryos of the Tuebingen strain were used. Embryos were incubated in Holtfreter's solution at 28.5°C.

Gene identification and construct generation

To identify Fgf-responsive genes, embryos were injected with 10 pg *fgf17b* mRNA or 100 pg *XFD* mRNA encoding a dominant-negative form of *Xenopus* Fgf receptor at the one-cell stage. RNAs were isolated from wild-type and injected embryos at the shield stage, respectively, and were labeled and hybridized to a zebrafish cDNA microarray as described before (Lo et al., 2003). The sample from wild-type embryos was used as a reference sample against which samples from injected embryos were compared. In two repeats, the cDNA #076-A05-2 showed an increase of expression level in *fgf17b*-injected samples with a logarithm ratio of 5.0

[1]State Key Laboratory of Biomembrane and Membrane Biotechnology, Department of Biological Sciences and Biotechnology, Tsinghua University, Beijing 100084, China. [2]Institut de Génétique et de Biologie Moléculaire et Cellulaire, CNRS/INSERM/ULP, 1, rue Laurent Fries, BP10142, 67404 Illkirch Cedex, France. [3]Institute of Molecular and Cell Biology, Proteos, 138673, Singapore.

*These authors contributed equally to this work
†Authors for correspondence (e-mail: thisse@titus.u-strasbg.fr; mengam@mail.tsinghua.edu.cn)

Accepted 14 December 2006

or 5.9, respectively. However, this cDNA showed a decrease of expression level in *XFD*-injected samples in two repeats, with a logarithm ratio of –3.3 or –2.35, respectively. Thus, this cDNA represented a gene positively regulated by Fgf signal.

Sequence analysis revealed that the cDNA clone #076-A05-2 contains 5′ partial sequence of putative *amotl2* cDNA. The other sequences of putative *amotl2* were cloned by RACE RT-PCR and ligated together. The *amotl2* cDNA sequence was deposited in GenBank with an accession number DQ887096. The full coding sequence of *amotl2* was amplified with a pair of primers (5′-GGAATTCCATATGAGAACGGCAG-AGGAATC-′3 and 5′-GTCCTCGAGTGGACATTGTTATCTCAGATG-3′) and subcloned into pCMV5-Myc, pCMV5-HA or pEGFP-N3 to generate mammalian expression constructs, or into pXT7 to generate a vector for synthesizing mRNA in vitro. For generating amotl2ΔPDZ constructs, another lower primer (5′-CGGGATCCTTAACTAC-TTTGCTCACCTTTGGC-3′) was used. For in vitro synthesizing *amotl2*^{m} mRNA that could not be targeted by amotl2MO1, a modified upper primer (5′-GGGGTACCACCATGCGTACCGCTGAAGAGAGCTCAGGAAC-GGAGCTGCACCG-3′) (substitutes underlined) was used for amplification of the *amotl2* coding sequence. To generate zebrafish amotl2ΔEILI that lack C-terminal 4 aa PDZ-binding domain, a specific upper primer (5′-GGAATTCCATATGAGAACGGCAGAGGAATC-3′) and a lower primer (5′-CTAGTCTAGATCACACCATGTCATTTT-CGACGG-3′) were used for PCR amplification. The coding sequence of human AMOTL2 was amplified from cDNAs derived from HeLa cells with an upper primer (5′-CGGAATTCATGAGGACACTGGAAGACTC-3′) and a lower primer (5′-CGGATATCGTCGACTCAGATCAGTATCT-CCACC-3′), which were designed based on human amotl2 sequence in GenBank (NM_016201). The lower primer for creating human AMOTL2ΔPDZ that lacks C-terminal 131 residues has a sequence of 5′-CGGATATCGTCGACTCAGGAGCGCTGCTGAAGG-3′. The coding sequences of zebrafish *c-src* (*csk* – Zebrafish Information Network), *fyn* and *yes* (*yes1* – Zebrafish Information Network) were individually subcloned into the expression vector pCMV5 using primers 5′-CCG-GAATTCCATATGGGTGGAGTCAAGAGTAA-3′ and 5′-CGCGGAT-CCCTAGAGGTTTTCTCCGGGTTG-3′ for *c-src*, 5′-CCGGAATTCC-ATATGGGCTGTGTGCAATGTAA-3′ and 5′-CGCGGATCCTTAGAG-GTTGTCCCCGGGTTG-3′ for *fyn*, and 5′-CCGGAATTCCATATGGG-CTGTGTCAAGAGTAA-3′ and 5′-CGCGGATCCCTACAGGTTGTCT-CCGGGCTG-3′ for *yes*.

RNA synthesis, morpholinos, microinjection, whole-mount in situ hybridization

Capped RNAs were synthesized using T7 or SP6 Cap Scribe (Roche) according to the manufacturer's instructions. Digoxigenin-UTP-labeled antisense RNA probes were generated by in vitro transcription and used for whole-mount in situ hybridization. Two antisense morpholinos, amotl2MO1 (5′-CTGATGATTCCTCTGCCGTTCTCAT-3′, positioning from 236-260 of *amotl2* sequence (DQ887096)) and amotl2MO2 (5′-CATTTCAGT-CTATGTTTAACAGACA-3′, positioning from 214-238 of *amotl2* sequence (DQ887096)), were synthesized by Gene Tools, LLC. A control morpholino (cMO1) has a sequence (5′-TACTCTTGCCGTCTCCTTAGTAGTC-3′) that is inverted from amotl2MO1. Amotl2MO1 and cMO1 were also synthesized with a 3′ carboxyfluorescein and a 3′ lissamine end modification, respectively. Unless otherwise stated, mRNAs and morpholinos were injected into yolk of fertilized eggs, and the dose was an estimate for the amount received by each embryo. Microinjection was performed as before (Zhao et al., 2003).

Cell culture, immunostaining and immunoprecipitation

Mammalian cells were grown in DMEM (GIBCO) supplemented with 10% fetal calf serum (Hyclone). When stimulation was required, the cells were starved for 24 hours and then treated with 100 nmol/l bradykinin (Sigma-Aldrich). Immunostaining, immunoblotting and co-immunoprecipitation were performed as before (Xiong et al., 2006; Zhang et al., 2004). For wound-healing assay, HEK293T or COS1 cells grown on glass slides were scratched with a sterile pipette tip, followed by transfection with corresponding plasmid DNAs. Rabbit polyclonal anti-c-Src, rabbit polyclonal anti-p-c-Src, rabbit polyclonal anti-RhoB and mouse monoclonal anti-EEA1 were purchased from Santa Cruz Biotechnology. TRITC-conjugated phalloidin was product of Molecular Probes. The secondary antibodies were products of Jackson ImmunoResearch Laboratories, Inc. Whole-mount in situ hybridizations were performed as described before (Thisse et al., 2004).

RESULTS

Zebrafish *amotl2* is an Fgf-responsive gene

In an effort to screen Fgf-responsive genes in the zebrafish embryo by cDNA microarray, we identified *amotl2* as one of cDNA clones that were upregulated in *fgf17b*-injected embryos but downregulated in FGF-deficient embryos (Fig. 1A). The large open reading frame of *amotl2* encodes a putative peptide of 721 residues with 55.2 and 54.5% of overall sequence identity to human AMOTL2 and mouse Amotl2, respectively. However, the putative peptide shares a sequence identity of 37 and 36.1% to human and mouse Amotl1, and of 34.1 and 29.2% to human and mouse Amot, respectively. The sequence homology analysis supports the notion that the putative peptide is a zebrafish homolog of mammalian Amotl2. Like human AMOTL2, zebrafish Amotl2 has a glutamine-rich domain (13-167 aa), the coiled coil domain (278-536 aa) and a PDZ-binding domain at the C-terminus (Fig. 1B), but it lacks a domain that is found in Amot and is bound by the angiogenesis inhibitor angiostatin (Bratt et al., 2002; Troyanovsky et al., 2001).

We investigated the spatiotemporal expression pattern of *amotl2* in zebrafish embryos by whole-mount in situ hybridization. *amotl2* transcripts were detected before the 1k-cell stage (Fig. 2A,B), suggesting that it is maternally supplied. At the sphere stage stronger staining was detected in the dorsal blastomeres (Fig. 2C); then *amotl2* transcripts were found in the whole gastrula, except in the evacuation zone, which corresponds to the ventral-animal territory of the embryo (Fig. 2D,E). During segmentation, *amotl2* is expressed in many distinct domains, including the polster, telencephalon, trigeminal placodes, rhombomeres, trunk neurons, somites and axial vasculature (Fig. 2F-J). The same expression pattern remains during the pharyngula period (Fig. 2K-O), except that *amotl2* is also expressed in lateral line primordia and in intersegmental vessels.

To confirm responsiveness of *amotl2* expression to Fgf signals, we injected embryos with *fgf8* mRNA and examined *amotl2* expression. Embryos injected at the one-cell stage expressed *amotl2* throughout the animal hemisphere at the shield stage (Fig. 2Q). When a single cell at the animal pole of an embryo at the 32- or 64-cell stage was injected with *fgf8* mRNA, *amotl2* expression was locally, strongly induced at the shield stage (Fig. 2R,S), indicating that ectopic Fgf signal is able to induce zygotic expression of *amotl2*. We also treated embryos with various doses of the Fgfr inhibitor SU5402, and examined *amotl2* expression at the 60% epiboly stage. As shown in Fig. 2T-W, progressive increase of SU5402 concentration caused *amotl2* expression to be progressively restricted to the most dorsal side of the gastrula embryo, showing that endogenous Fgf signaling is required for zygotic expression of *amotl2* in ventral and lateral marginal cells.

Knockdown of *amotl2* expression inhibits cell migration during embryogenesis

To study functions of endogenous *amotl2* in development of zebrafish embryos, we used two antisense morpholino oligonucleotides, amotl2MO1 and amotl2MO2, which target different sequences of *amotl2*, to block translation of *amotl2* mRNA. Both morpholinos effectively inhibited production of the Amotl2-

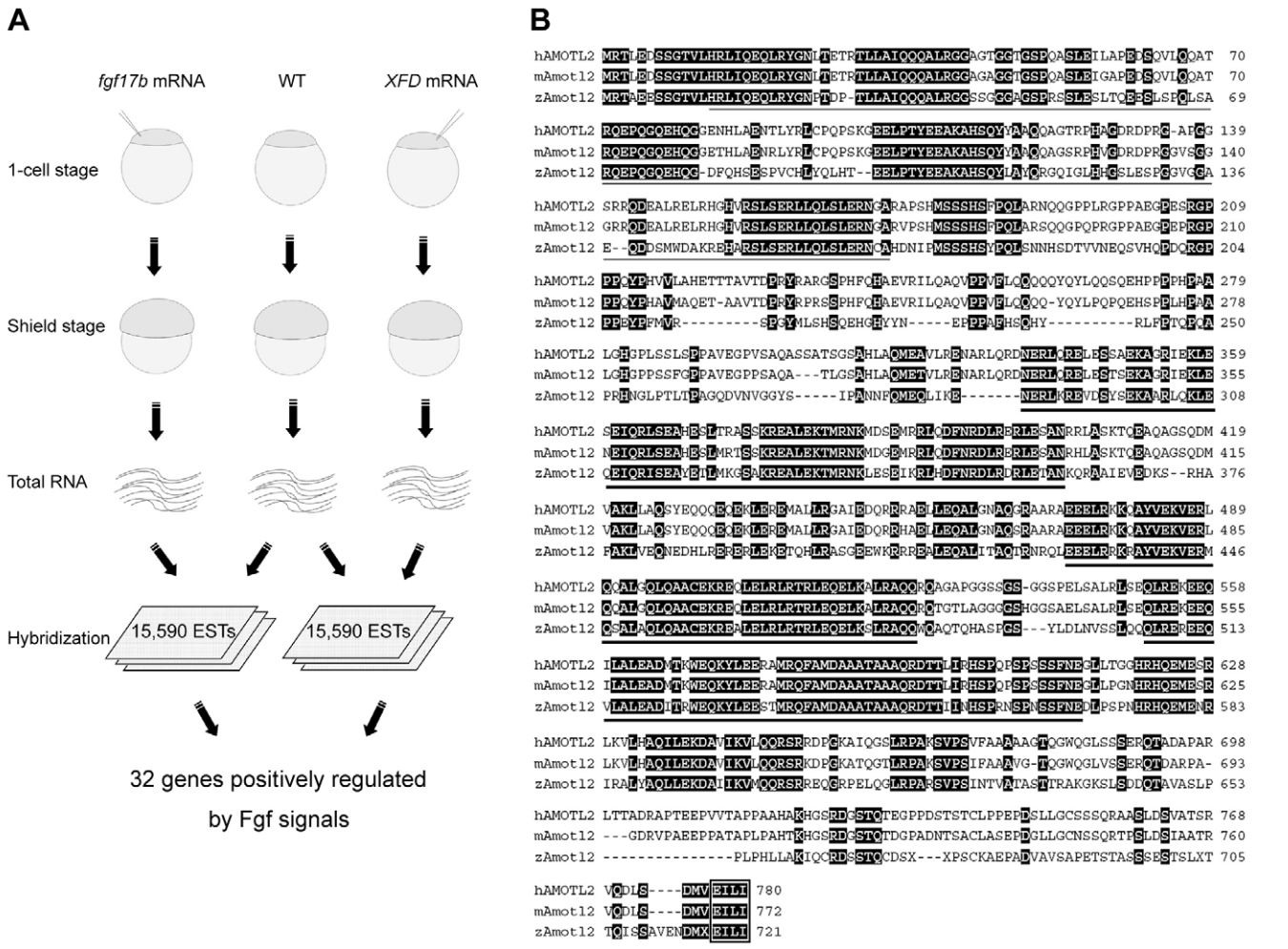

Fig. 1. Identification of zebrafish *amotl2* and sequence alignment of Amotl2 proteins. (**A**) Schematic illustration of procedures for identification of Fgf-responsive genes. One-cell embryos were injected with 10 pg *fgf17b* mRNA or 100 pg *XFD* mRNA that encodes a dominant-negative form of *Xenopus* Fgfr1. The injected embryos and uninjected embryos were collected at the shield stage for total RNA extraction. mRNAs were isolated from the total RNAs and used for making fluorescent probes. The fluorescent probes were hybridized to cDNAs arrayed in slides. A cDNA was regarded as an Fgf-responsive gene if the signal ratio between *fgf17b*-injected and wild-type embryos or between *XFD*-injected and wild-type embryos is greater than twofold. (**B**) Sequence alignment of human, mouse and zebrafish Amotl2 proteins. The number on the right of each line indicates the position of the last residue on the line. The coiled coil domains are underlined with thick lines; the glutamine-rich domain is underlined with a thin line; and the PDZ-binding domain at the C-terminus is boxed. The conserved residues were shadowed. Human AMOTL2 (hAMOTL2) and mouse Amotl2 (mAmotl2) sequences were derived from GenBank with accession numbers NP_057285 and Q8K371, respectively.

GFP fusion protein in zebrafish embryos, while the control morpholino cMO1 had no effect (Fig. 3). Because amotl2MO1 is more effective than amotl2MO2, we used amotl2MO1 only in most of our experiments. Compared to wild-type or cMO1-injected embryos, embryos injected with amotl2MO1 showed slower epiboly in a dose-dependent manner (Fig. 4A). When wild-type or cMO1-injected embryos developed to the bud stage [10 hours post-fertilization (hpf)], for instance, embryos injected with 1, 2, 3, 4 or 5 ng of amotl2MO1 developed to approximately 100, 95, 75, 70 or 55% epiboly stages, respectively. Close examinations at higher magnifications revealed that movements of enveloping layer, deep cells, forerunner cells and yolk syncytial layer were slower in amotl2MO1-injected embryos (data not shown). At the five- to six-somite stage (~12 hpf), wild-type embryos have a long anteroposterior embryonic axis around the yolk due to convergent extension (CE) movements. At this stage, by contrast, embryos injected with 1-3 ng amotl2MO1 had a shorter embryonic axis, albeit the epiboly was complete, suggesting impaired extension movement; and embryos injected with 4 or 5 ng amotl2MO1 died without completion of epiboly. Injection with 30 ng amotl2MO2 similarly delayed epiboly and impaired extension, implying that targeting effect of both morpholinos should be specific.

To confirm effect of *amotl2* morpholino injection on CE movements, we examined the expression of a set of marker genes that have been used to reflect CE movement (Marlow et al., 2002; Topczewski et al., 2001). In wild-type embryos at the two-somite stage, the neural plate, boundaries of which are marked by *dlx3* expression, become narrow, and the polster, which is derived from the anterior hypoblast cells and expresses *hgg1* (*ctslb* – Zebrafish Information Network), is positioned in front of the anterior edge of

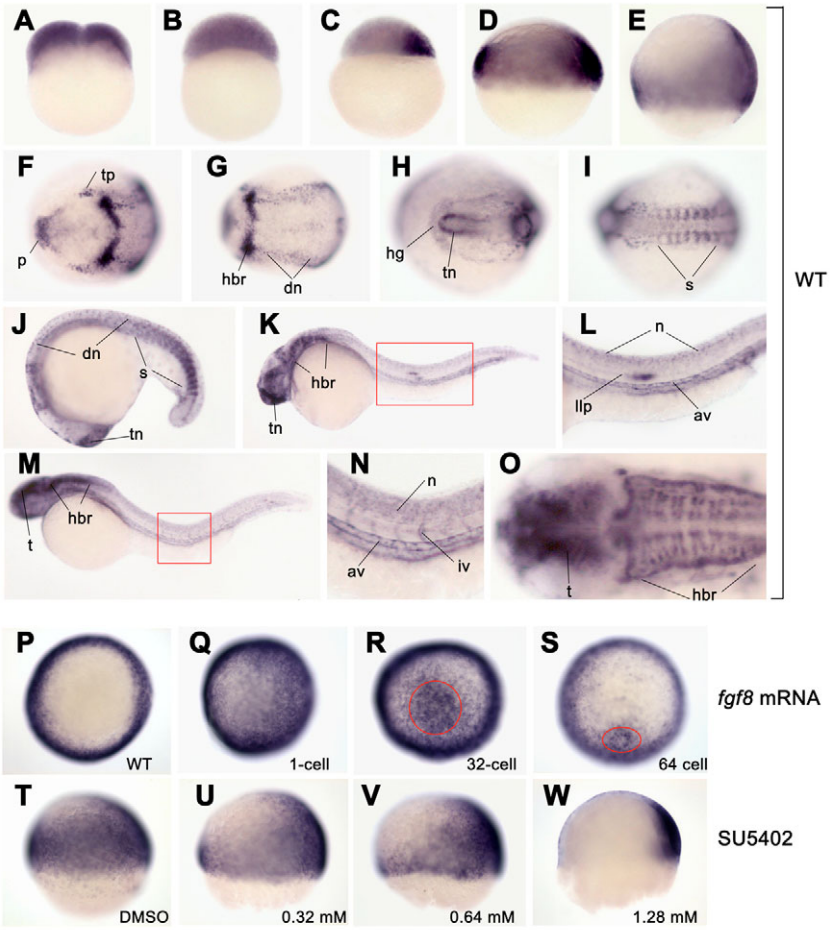

Fig. 2. *amotl2* expression and regulation by Fgf signal in zebrafish embryos. (**A-O**) *amotl2* expression in wild type was detected by whole-mount in situ hybridization at two-cell (A), 1k-cell (B), sphere (C), shield (D), 70% epiboly (E), two-somite (F,G), ten-somite (H,I), 18-somite (J), 24 hpf (K,I) and 36 hpf (M-O) stages. (A-E) Lateral views with dorsal to the right; (F-I,O) dorsal views with anterior to the left; (J-N) lateral views with anterior to the left. (F and G; H and I) The anterior (F,H) and posterior (G,I) regions for the same embryo, respectively. (L) Higher magnification of the region boxed in K. (N) Higher magnification of the region boxed in M. (O) Head of the embryo in M. (**P-W**) *amotl2* expression in embryos injected with 14 pg *fgf8* mRNA (Q-S) or treated with Fgfr signaling inhibitor SU5402 (U-W). (P-S) Animal pole views at the shield stage with dorsal to the right. (T-W) Lateral views at the 60% epiboly stage with dorsal to the right. *fgf8* mRNA was injected into a one-cell embryo (Q) or a single cell located in the animal pole at the 32-cell stage (R) or the 64-cell stage (S). *amotl2* expression was strongly induced in the circled area following single-cell injection at multi-cell stages (R,S). SU5402 treatment started at the sphere stage. av, axial vasculature; dn, dorsal neuron; hbr, hindbrain rhombomere; hg: hatching gland; iv, intersegmental vessel; llp, lateral line primordium; n, neuron; p, polster; s, somite; t, tectum; tn, telencephalon; tp, trigeminal placodes; vn, ventral neuron.

the neural plate (Fig. 4B). In embryos injected with amotl2MO1 at the same stage, by contrast, the neural plate was much broader and the polster was seated within or fell behind the anterior edge of the neural plate. It is also apparent that injection with amotl2MO1 or amotl2MO2 resulted in shorter, but wider *ntl* expression domain, or unmerged stripes (Fig. 4B). These observations further support the notion that knockdown of *amotl2* expression affects CE movements during zebrafish embryogenesis. Additionally, most of the amotl2MO1-injected embryos showed dorsalized phenotypes (data not shown), suggesting an involvement of *amotl2* in embryonic patterning. It is possible that the observed convergence and extension defects might be due to requirement of *amotl2* for cell motility as well as for embryonic patterning.

To investigate the effects of *amotl2* overexpression, we injected single-cell embryos with 100~900 pg *amotl2* mRNA and found no obvious morphological changes (data not shown). Then we tested whether *amotl2* overexpression could rescue amotl2MO1-induced defects in cell movement. Because the amotl2MO1 sequence is complementary to the first 25 nucleotides of the *amotl2* coding sequence, we made base substitutions in that region so that the resulting *amotl2*^{m} mRNA could not be bound by amotl2MO1 while the residue identities were not changed. Embryos injected with 600 pg *amotl2*^{m} mRNA alone did not show any defects (Fig. 4B,C). When injected with 3 ng amotl2MO1 alone, 16.1% (n=93) of embryos never completed epiboly and 75.3% of embryos showed epiboly and/or CE defects at the bud and seven-somite stages (Fig. 4C). When amotl2MO1 and *amotl2*^{m} mRNA were co-injected, 50% of embryos (n=96) exhibited slightly slower epiboly at the bud stage and less severe CE defects at later stages, while the other embryos looked normal (Fig. 4C). Thus, *amotl2* overexpression can compromise the effect of knockdown of *amotl2* expression, further suggesting that *amotl2* is essential for normal epiboly and CE movements of zebrafish embryos.

We injected a fluorescein-labeled amotl2MO1 (green) or a lissamine-labeled cMO1 (red) into a single blastomere at the 64-cell stage, and subsequently analyzed the migration behavior of the derived clone. The injected embryos were sorted out at the shield stage, based on locations of the labeled progeny cells, into three groups: dorsal, lateral and ventral, and further observed during early segmentation (five- to ten-somite stages) and at 24 hpf (Fig. 5A). When control cMO1 was injected, labeled cells migrated according to their positions on the fate map for more than 70% of embryos at 24 hpf: dorsal clones colonizing the head, lateral clones colonizing posterior head and trunk, and ventral clones populating the tail region. When amotl2MO1 was injected, labeled cells failed to migrate and clustered on the yolk in more than 80% of embryos at 24 hpf. Analysis of cell death, using the vital dye Nile Blue Sulfate (Dupe et al., 1999), revealed that clustering of amotl2MO1-injected cells on the yolk at 24 hpf was not correlated with cell death (data not shown), excluding the possibility that the morpholino has a lethal effect. It is likely that Amotl2-deficient cells lose migratory ability and are pushed out to the yolk surface. In addition, our data suggest that *amotl2*-mediated migration is a cell-autonomous effect.

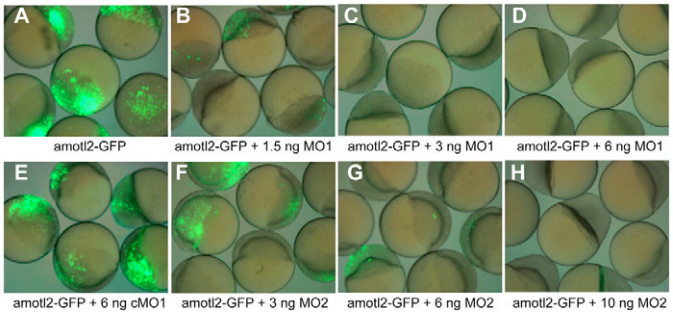

Fig. 3. Effectiveness of *amotl2* morphants. Embryos injected with 50 pg amotl2-GFP plasmid DNA showed green fluorescence at the shield stage (**A**). When co-injected with amotl2MO1 (MO1) or amotl2MO2 (MO2), green fluorescence decreased in a dose-dependent way (**B-D**,**F-H**). However, co-injection with cMO1 did not inhibit production of Amotl2-GFP fusion protein (**E**). Note that a higher dose of MO2 was required to inhibit Amotl2-GFP expression.

Knockdown of *amotl2* expression disrupts membrane protrusion and actin filaments

To look into the effects of knockdown of *amotl2* expression on membrane protrusions, we co-injected the morpholino together with an mRNA coding for a membrane-targeted GFP into one blastomere at the 64-cell stage and observed by confocal fluorescent microscopy at the end of gastrulation (Fig. 5B). Cells injected with the membrane GFP mRNA alone or in combination with 4 ng cMO1 had ruffles on the surface, including filopodia, while cells co-injected with the membrane GFP mRNA and 4 ng amotl2MO1 were rounded, with few filopodia. The number of protrusions per cell was 7.4±0.5 for membrane GFP injection (average for 30 cells of five embryos), 8.2±0.8 for cMO1 injection (average for 38 cells of five embryos), and 0.65±0.3 for amotl2MO1 injection (average for 47 cells of nine embryos). These results indicate that *amotl2* is required for formation of membrane protrusion. Given that microfilaments play important roles in cell migration, we examined by phalloidin staining the distribution of actin filaments in embryonic cells following *amotl2* expression knockdown. As shown in Fig. 5C, juxtamembrane actin fibers were less abundant and discontinuous in the epiblast cells of amotl2MO1-injected embryos at the shield stage, compared with those in cMO1-injected embryos. These data suggest that *amotl2* is required for formation and ordered array of actin filaments during early embryogenesis.

Deletion of PDZ-binding domain converts Amotl2 into a dominant-negative form

It has been found that overexpression of mutant Amot with deletion of the C-terminal PDZ-binding domain inhibits cell migration in vitro (Troyanovsky et al., 2001) and in mouse embryos (Levchenko et al., 2003). During cloning of the 3′ end sequence of zebrafish *amotl2* by RACE-PCR, we obtained an intermediate *amotl2* cDNA, *amotl2ΔPDZ*, which lacks sequence encoding the C-terminal 117 residues that includes the putative PDZ-binding domain. We injected *amotl2ΔPDZ* mRNA, side by side with full-length *amotl2* mRNA, into single-cell embryos and observed morphological changes during gastrulation and early segmentation. When the tailbud formed in wild-type or *amotl2* mRNA-injected embryos, the yolk plug in *amotl2ΔPDZ*-injected embryos (69/79) had not been completely covered by the blastoderm (Fig. 6A), suggesting that overexpression of *amotl2ΔPDZ* leads to a slower epiboly process. During the early segmentation period, the distance between the rostral and caudal ends of the embryonic axis on the ventral side was longer in *amotl2ΔPDZ*-injected embryos than in wild-type embryos, being indicative of an extension defect. We then examined expression of *hgg1*, *dlx3* and *ntl* in injected embryos. As shown in Fig. 6B, overexpression of *amotl2ΔPDZ* resulted in wider neural plate (marked by *dlx3*), wider but shorter notochord (marked by *ntl*), and slower migration of the anterior prechordal plate (marked by *hgg1*) in 66.1% (n=56) of *amotl2ΔPDZ*-injected embryos, suggesting defective CE movements. Taken together, the effects of *amotl2ΔPDZ* overexpression on embryonic cell movements resemble those of amotl2MO1 injection, suggesting that Amotl2ΔPDZ has a dominant-negative effect on endogenous Amotl2 activity. To confirm Amotl2 function in cell movements is absolutely mediated by its C-terminal PDZ-binding domain (EILI motif), we made an amotl2ΔEILI mutant that lacks only four residues (EILI) at the C-terminus. Injection of 400 pg *amotl2ΔEILI* mRNA caused defects in convergent extension in 52.5% (n=40) of embryos (Fig. 6B), which confirms the requirement of the EILI motif for normal function of Amotl2. In another experiment, co-injection of 400 pg *amotl2ΔEILI* mRNA with equal amount of wild-type *amotl2* mRNA led to only 30% (n=60) of embryos with convergent extension defects, compared with 49.1% (n=57) of embryos with the same phenotypes that were injected with 400 pg *amotl2ΔEILI* mRNA alone. This result suggests that Amotl2ΔEILI interferes with the function of wild-type Amotl2.

We further tested the effects of Amotl2ΔPDZ on cell migration in mammalian cells by wound-healing assay. HEK293T and COS1 cells were transfected with pEGFP-N3, pAmotl2-EGFP or pAmotl2ΔPDZ-EGFP and scratches were made. Twenty-four hours after wounding, the number of GFP-positive cells in the wound areas was counted. We found that transfection with pAmotl2-EGFP promoted migration of cells into the wound area, whereas transfection with pAmotl2ΔPDZ-EGFP inhibited such migration (Fig. 6C). However, neither Amotl2-EGFP nor Amotl2ΔPDZ-EGFP influenced cell proliferation in NIH3T3 cells (data not shown). These results further confirm that the mutant form Amotl2ΔPDZ plays an inhibitory role in cell migration.

To investigate the effects of Amotl2ΔPDZ overexpression on distribution of actin filaments, Myc-Amotl2ΔPDZ, which was derived from zebrafish Amotl2, or HA-AMOTL2ΔPDZ, which was derived from human AMOTL2, was transfected into HeLa cells and F-actin was stained with phalloidin. As shown in Fig. 6D, overexpression of either mutant Amotl2 resulted in less abundance and disruption of peripheral F-actin. This result is consistent with the observation in zebrafish embryos injected with amotl2MO1 (Fig. 5C). In addition, most cells (82%) overexpressing the mutant Amotl2 looked rounded with a cell length:width ratio of less than 2:1, while only 16% of cells overexpressing wild-type Amolt2 had a similar shape.

Amotl2 binds to and promotes translocation of c-Src

The non-receptor tyrosine kinase Src plays important roles in actin cytoskeleton remodeling and cell motility by phosphorylating various substrates (Frame, 2004; Ishizawar and Parsons, 2004). As Amotl2 also affects these aspects, we asked if Amotl2 interacted with Src. To test interaction between fish Amotl2 and exogenous c-Src, HA-Amotl2 was co-transfected with GFP-tagged wild-type (Src-WT-GFP) or constitutively active mutant c-Src (Src-Y527F-

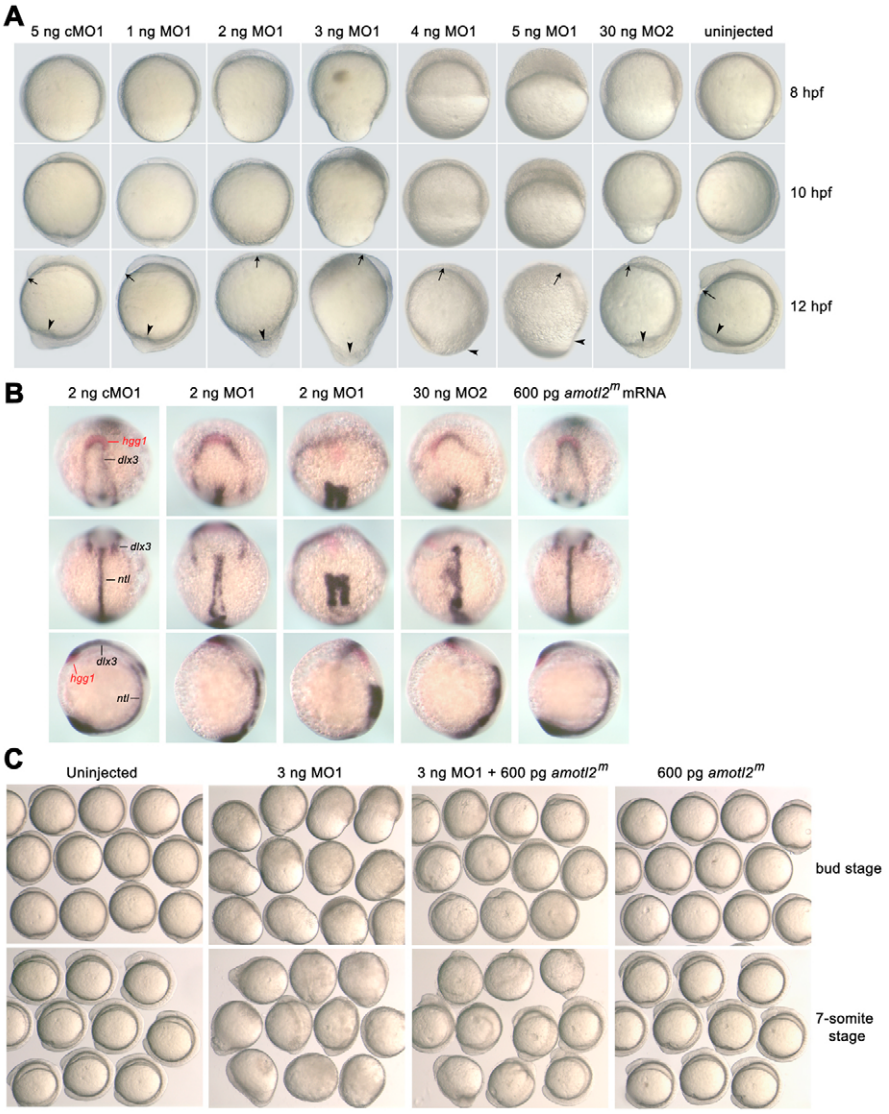

Fig. 4. Effects of *amotl2* expression knockdown on embryonic cell movements. (**A**) Injection of *amotl2* morpholino led to slower epiboly and impaired CE movement. Single-cell embryos were injected with amotl2MO1 (MO1), amotl2MO2 (MO2) or control morpholino (cMO1) at the indicated doses. The same embryo was pictured every 2 hours and presented here. Embryos are shown as lateral views with animal pole to the top and dorsal to the right. Arrows denote the anterior tip of the hypoblast, and arrowheads point to the tail region. (**B**) Injection of *amotl2* morpholino affected convergent extension. Injected embryos at the two-somite stage were fixed and simultaneously hybridized to *hgg1* (red), *dlx3* (blue) and *ntl* (blue) probes. Each embryo was placed in different orientation: in the top panel, anterodorsal views show relative positions of the *hgg1* and *dlx3* domains; in the middle panel, dorsal views show the *ntl* domain; and in the bottom panel, lateral views with dorsal to the right show the length of the *ntl* domain and the embryonic anteroposterior axis. (**C**) Effect of *amotl2* morpholino injection was alleviated by overexpression of modified *amotl2* (*amotl2*^{m}) mRNA. Groups of live embryos were pictured at the indicated stages.

GFP) (Sandilands et al., 2004) into human HEK293T cells. In the precipitates pulled down with anti-GFP antibody, Amotl2 was detected by anti-HA immunoblotting, suggesting that Amotl2 can bind to both wild-type and active c-Src with higher affinity to the active form (Fig. 7A). In a reciprocal experiment with anti-HA immunoprecipitation and anti-GFP immunoblotting, the Amotl2/c-Src complexes were not detected, which might result from mask of the GFP epitope by anti- HA antibody in the complexes. Then, we tested interaction between Amotl2 and endogenous c-Src in HEK239T cells. In the precipitates pulled down with anti-HA antibody, endogenous c-Src was detected by anti-Src antibody (Fig. 7B), indicating that overexpressed Amotl2 physically binds to endogenous c-Src. Furthermore, immunostaining showed that HA-Amotl2 co-localized with Src-WT-GFP or endogenous c-Src in mammalian cells (Fig. 7C). Taken together, these data indicate that Amotl2 can form complexes with c-Src. Fyn and Yes are also Src family protein tyrosine kinases (Thomas and Brugge, 1997), and have been found to play a role in convergent extension cell movements during gastrulation of zebrafish embryos (Jopling and den Hertog, 2005). We tested whether Amotl2 could also physically associate with Fyn and Yes. When Myc-Amotl2 was coexpressed with HA-Fyn or HA-Yes in HEK293T cells, reciprocal co-immunoprecipitation failed to detect Myc-Amotl2/HA-Fyn or Myc/HA-Yes complexes (Fig. 7D). This suggests that Amotl2 is unable to bind Fyn or Yes.

Src is translocated from the perinuclear region to the peripheral cell-matrix adhesions to exert its biological effects (Fincham et al., 1996; Kaplan et al., 1992; Timpson et al., 2001). We investigated the possible involvement of Amotl2 in peripheral targeting of Src in HeLa cells using the construct Src-Y527F-GFP. As shown in Fig. 7E, treatment with bradykinin induced translocation of Src-Y527F-GFP to filopodia and lamellipodia. In cells co-transfected with Myc-Amotl2, Src-Y527F-GFP was also targeted, following bradykinin stimulation, to filopodia with the farthest ends beyond those of Amotl2. When Src-Y527F-GFP was co-transfected with Myc-Amotl2ΔPDZ, however, Src-Y527F-GFP reached the cell periphery and stopped at the base of filopodia. We then examined distribution of endogenous phosphorylated c-Src in cells transfected with Myc-Amotl2 or Myc-Amotl2ΔPDZ using antibody against phospho-c-Src (Thr420). We found that phospho-c-Src was abundant at the

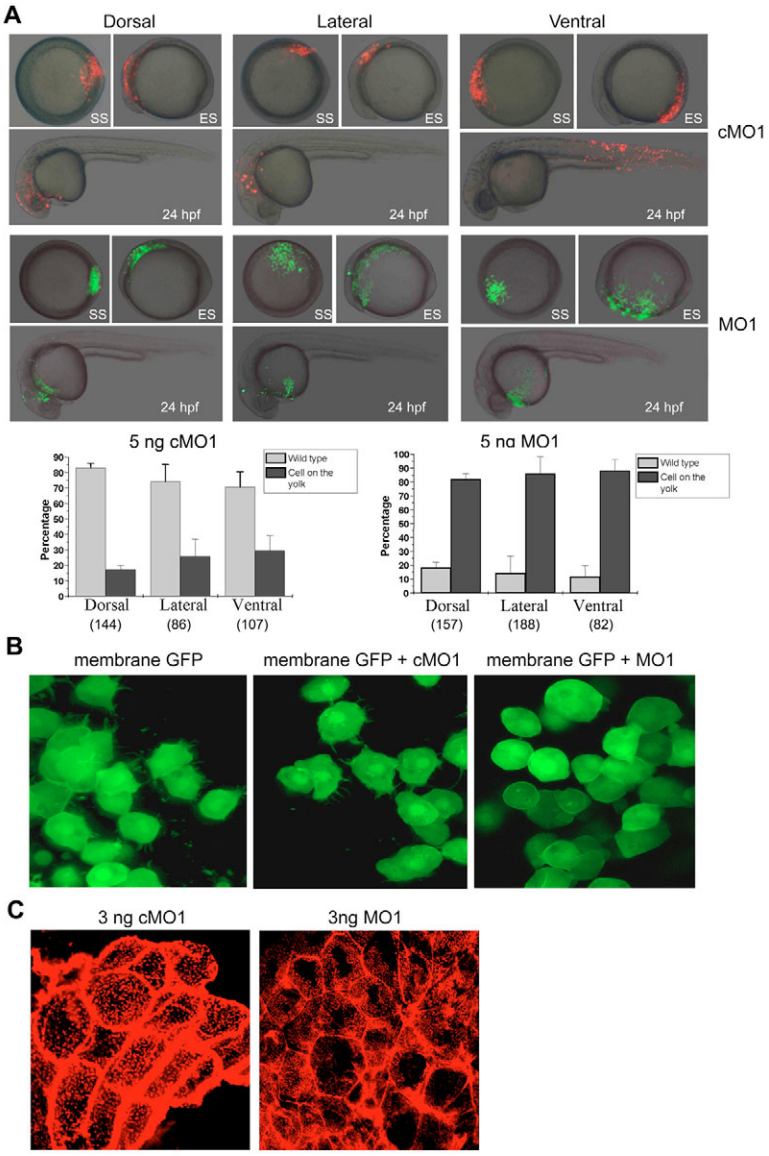

Fig. 5. Effects of *amotl2* expression knockdown on cell movements and structures. (**A**) Migratory behavior of clonal cells. One cell of a 64-cell embryo was injected with lissamine-labeled control MO1 (cMO1) or fluorescein-labeled amotl2MO1 (MO1). According to location of labeled descendants at the shield stage (SS), embryos were separated into three groups: dorsal, lateral and ventral. The sorted embryos were observed again during early segmentation (ES) and at 24 hpf. Cells targeted by cMO1 contributed to corresponding embryonic tissues at 24 hpf (upper panel), while MO1-targeted cells mainly clustered on the yolk at 24 hpf regardless of their early locations (lower panel). The bar graphs show percentage of embryos with labeled cells in embryonic tissues (wild type) or on the yolk based on four independent experiments. The total number of observed embryos is indicated in parentheses. (**B**) Effect of *amotl2* expression knockdown on cell shape. One cell of a 64-cell embryo was injected with 10 pg mRNA coding for membrane GFP alone or in combination with either 5 ng cMO1 or MO1. The labeled cells were observed at the end of gastrulation by confocal microscopy. Compared to the wild-type or cMO1-injected cells, MO1-injected cells had a round shape and lost membrane protrusions such as filopodia. (**C**) Effect of *amotl2* expression knockdown on F-actin. Embryos were injected with corresponding morpholinos at the one-cell stage and subsequently stained at the shield stage with phalloidin. Outer layer cells of flat-mounted embryos were photographed. Notice that, in MO1-injected cells, F-actin is less abundant in the peripheral region and not well ordered intracellularly.

periphery of cells transfected with Myc-Amotl2 but less abundant at the periphery of cells transfected with Myc-Amotl2ΔPDZ (Fig. 7F). These data suggest that overexpression of the mutant Amotl2 inhibits membrane translocation of activated c-Src.

Peripheral membrane translocation of c-Src is dependent on RhoB-containing endosomes that harbor proteins involved in actin polymerization and filament assembly (Sandilands et al., 2004; Timpson et al., 2001). We found that overexpressed Myc-Amotl2 was well co-localized with endogenous RhoB in HeLa cells and was also present in some of EEA1-positive endosomes (Fig. 7G). This observation supports the hypothesis that Amotl2 binds to and promotes translocation of c-Src to focal adhesions through RhoB-containing endosomes.

DISCUSSION

Amot, Amotl1 and Amotl2 constitute a new Motin family (Bratt et al., 2002). The founding member, Amot, has been identified as an angiostatin-binding partner (Troyanovsky et al., 2001). Amot promotes motility of endothelial cells, which is inhibited by Angiostatin. *Amot* homozygous mutant mice die soon after gastrulation due to abnormal movement of visceral endoderm (Shimono and Behringer, 2003). However, little is known about biological functions of Amotl1 and Amotl2. In this study, we demonstrate that *amotl2* is required for cell movements in zebrafish embryos. In vitro and in vivo analyses reveal that loss of the C-terminal PDZ-binding motif of Amotl2 inhibits cell migration, an effect also observed in Amot with deletion of the PDZ-binding motif (Levchenko et al., 2003; Troyanovsky et al., 2001). Thus, both Amot and Amotl2 have the ability to promote cell migration and are required for embryonic cell movements. Although functions of Amotl1 have not been reported, it may also be capable of promoting cell migration, as its sequence shares a high degree of homology with those of Amot and Amotl2 (Bratt et al., 2002). An interesting question is whether different members of the Motin family play redundant roles in embryonic cell movements. Examination of spatiotemporal expression patterns of different members will certainly provide clues.

In zebrafish embryos, knockdown of *amotl2* expression caused disordered array of juxtamembrane actin fibers and loss of filopodia and lamellipodia. Several lines of evidence from in vitro experiments

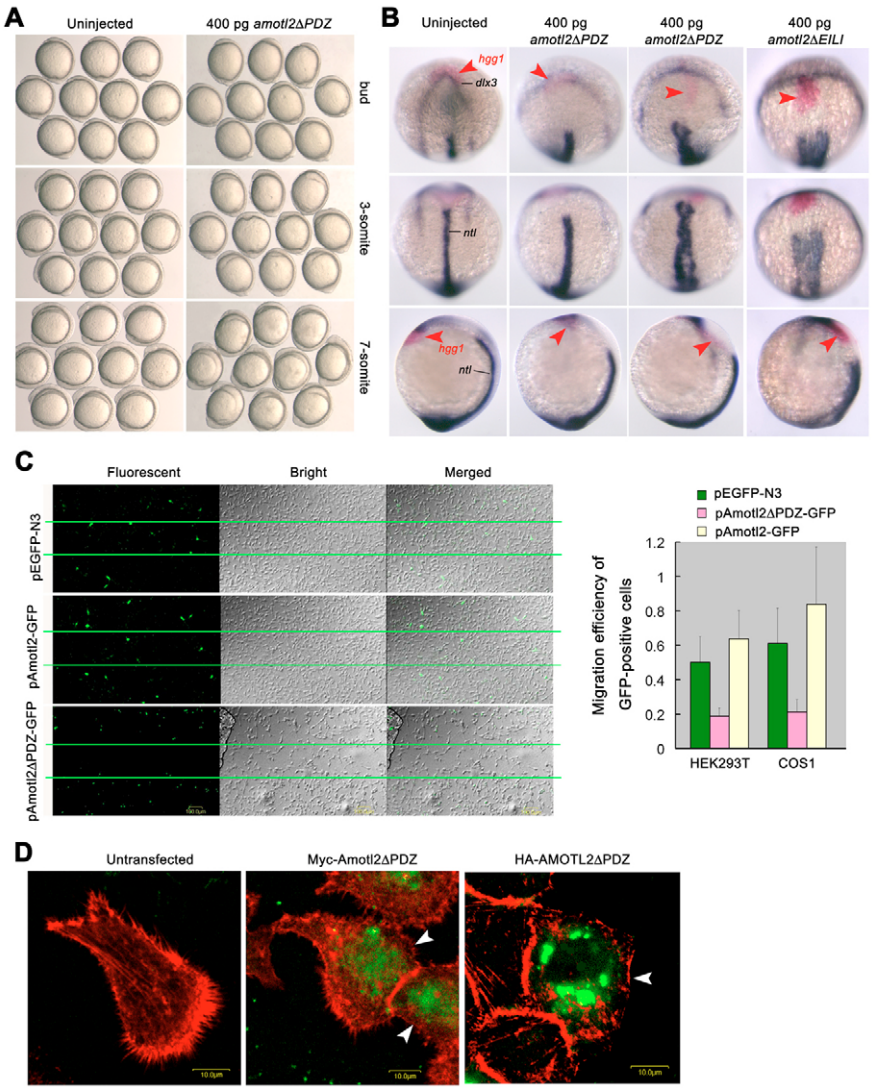

Fig. 6. Effect of *amotl2* mutants on cell migration and structures. (**A**) Effect of overexpression of *amotl2ΔPDZ* mutant on cell movements of zebrafish embryos. Embryos were injected at the one-cell stage and observed at the indicated stages. Embryos were managed to position with animal pole or anterior to the top. (**B**) Expression of *hgg1* (red), *dlx3* (blue) and *ntl* (blue) at the two-somite stage. Top panel, anterodorsal views; middle panel, dorsal views with anterior to the top; bottom panel, lateral views with anterior to the top and dorsal to the right. Injection of *amotl2ΔPDZ* mRNA led to varying degrees of defects in convergent extension (in the second and third columns). Injection of *amotl2ΔEILI* mRNA also caused defective convergent extension (fourth column). The *hgg1* expression domain is indicated by arrowheads. (**C**) Expression of Amotl2ΔPDZ-GFP or Amotl2-GFP inhibited or promoted cell migration in vitro, respectively. Wound-healing assays were done both in HEK293T (shown on the left) and in COS1 cells. The wound area was between two lines. The bar graph at the right shows statistical data from three experiments with standard deviations. The migration efficiency of GFP-positive cells was calculated as percentage of GFP-positive cells in the wound-healing area/percentage of GFP-positive cells in the non-wound area. (**D**) F-actin distribution was abnormal in HeLa cells transfected with either Myc-Amotl2ΔPDZ (derived from fish) or HA-AMOTL2ΔPDZ (derived from human). Cells were stained with phalloidin 24 hours after transfection. Arrowheads indicate Amotl2-expressing cells. Scale bars: 10 μm.

support the hypothesis that Amotl2 promotes cell migration, at least in part, by facilitating peripheral translocation of phosphorylated c-Src via endosomes. First, Amotl2 is co-localized with RhoB-positive endosomes that have been reported to be required for translocation of activated c-Src to focal adhesion complexes (Sandilands et al., 2004). Second, Amotl2 physically associates with c-Src with stronger affinity for phosphorylated c-Src, and largely co-localizes with c-Src. Third, overexpression of Amotl2ΔPDZ blocks membrane targeting of activated c-Src. c-Src regulates cell motility by interacting with and modulating numerous cellular factors that modulate cell surface structure, cell-cell adhesion and actin cytoskeleton (Frame, 2004; Huttelmaier et al., 2005; Ishizawar and Parsons, 2004; Nelson and Nusse, 2004). Thus, Amotl2 may promote cell migration through c-Src in multiple mechanisms. However, it remains to be elucidated whether c-Src relays Amotl2 function in cell movements in vivo.

The C-terminal PDZ-binding motif of Amotl2 is indispensable to its promoting effects on cell migration. The presence of this PDZ-binding motif provides an opportunity to interact with different PDZ domain scaffold proteins that can target cargoes to specific cell surface or subcellular compartments (Nourry et al., 2003). For example, we found through yeast two-hybrid screening that Amotl2 could bind to the PDZ-domain-containing protein MAGI-3, a member of the membrane associated guanylate kinase (MAGUK) family (data not shown). MAGUK proteins are located at the plasma membrane of epithelial cells and are involved in regulation of cell polarity and cell-cell adhesion by interacting with various proteins (Funke et al., 2005). We also found that Amotl2 is able to associate with the glutamate receptor interacting protein 1 (GRIP1). GRIP1 contains multiple PDZ domains, and it can bind to the cytoplasmic domain of Ephrin B1 and may serve as a scaffold for the assembly of multiprotein signaling complexes within specific membrane domains (Bruckner et al., 1999). Thus, Amotl2 may play roles in cell migration in the c-Src-dependent way as well as in c-Src-independent ways.

In this study, *amotl2* has been identified as an Fgf-responsive gene. Fgf signals have been found to play roles in cell movements during gastrulation of vertebrate embryos (Ciruna and Rossant, 2001; Nutt et al., 2001; Yang et al., 2002). We tested genetic interaction between Fgf signaling and *amotl2*. We found that overexpression of either *fgf17b* mRNA or dominant-negative *fgfr1* mRNA failed to rescue defective cell movements caused by loss of function of *amotl2* in zebrafish embryos (data not shown). It is likely that *amotl2* directly mediates activity of Fgf signaling and it also

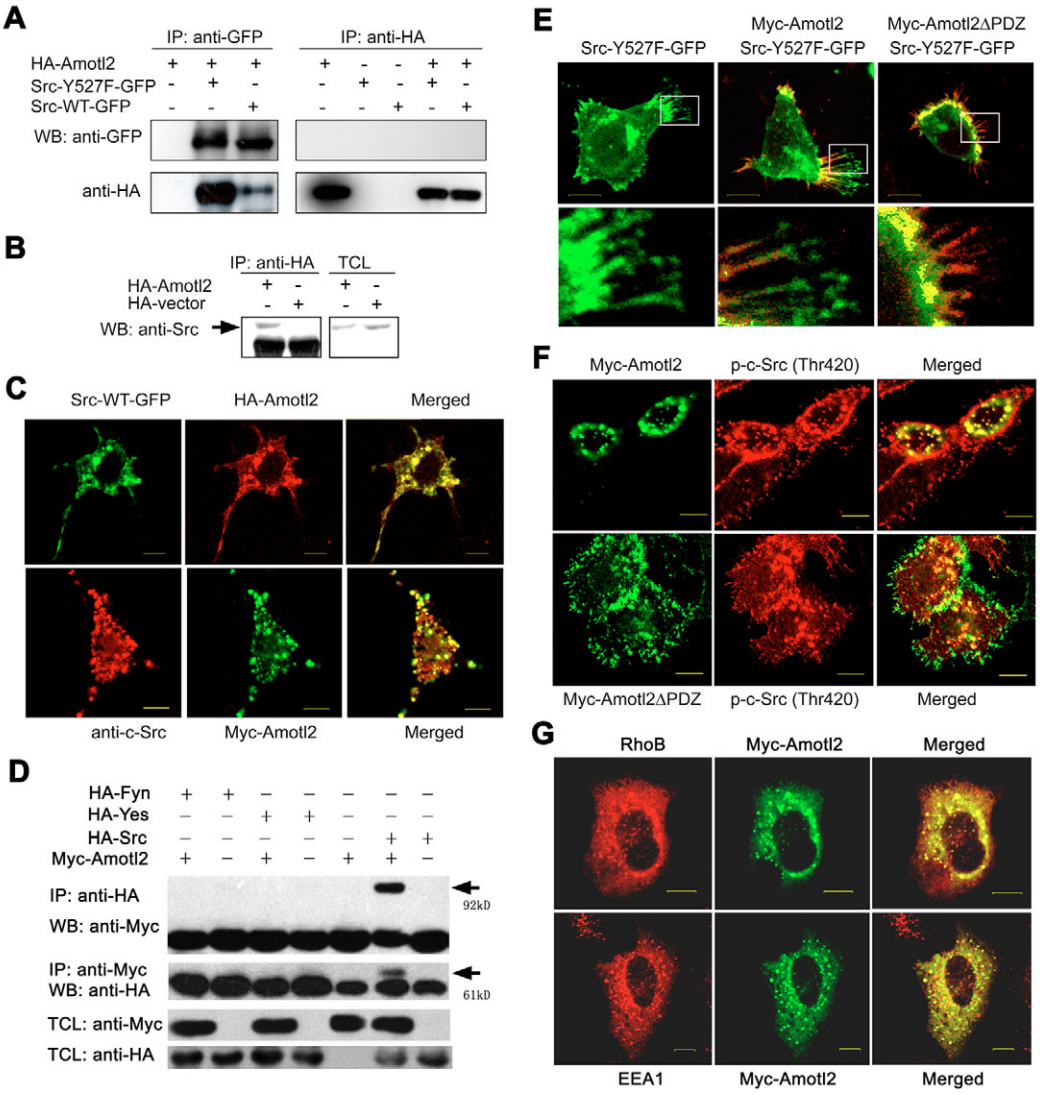

Fig. 7. Amotl2 associates with and promotes peripheral translocation of c-Src. (**A**) HA-Amotl2 was coexpressed with Src-WT-GFP or Src-Y527F-GFP in HEK293T cells and their interaction was examined by reciprocal immunoprecipitation. (**B**) Overexpressed HA-Amotl2 associated with endogenous c-SRC in human HEK293T cells. HA-Amotl2 was immunoprecipitated with anti-HA antibody and the precipitates were examined by western blotting for the presence of c-Src (indicated by an arrow) with anti-c-Src antibody. TCL, total cell lysate. (**C**) Overexpressed HA-Amotl2 or Myc-Amotl2 was co-localized with overexpressed Src-WT-GFP (upper panel) or endogenous c-Src (lower panel) in HeLa cells. (**D**) Examination of Amotl2 association with related tyrosine kinases Fyn and Yes of zebrafish. Myc-Amotl2 was coexpressed with HA-Src, HA-Fyn or HA-Yes in human HEK293T cells. Reciprocal co-immunoprecipitation was performed. Note that Myc-Amotl2 was co-precipitated with HA-Src (indicated by arrows), but not with HA-Fyn or HA-Yes. (**E**) Effect of Amotl2 on translocation of exogenous active c-Src. HeLa cells were transfected with Src-Y527F-GFP alone, or in combination with Myc-Amotl2 or Myc-Amotl2ΔPDZ, and treated with bradykinin. Lower panel: high magnification of an area boxed in the corresponding cell in the upper panel. (**F**) Effect of Amotl2 on translocation of endogenous phosphorylated c-Src in HeLa cells. Following transfection with Myc-Amotl2 (upper panel) or Myc-Amotl2ΔPDZ (lower panel), cells were treated with bradykinin and stained with p-c-Src (Thr420) antibody. (**G**) Co-localization of Myc-Amotl2 with endogenous endosomal proteins RhoB (upper panel) and EEA1 (lower panel) in HeLa cells. Scale bars: 10 μm.

exerts effects through other signaling pathways. The potential roles of Amotl2 in Fgf signaling and the underlying mechanisms need to be investigated in the future.

We are grateful to Dr Margaret C. Frame for providing plasmids Src-WT-GFP and Src-Y527F-GFP, and Dr Jeroen den Hertog for providing plasmids zebrafish fyn and yes. We also thank Yanning Rui for technical assistance. This work was supported by grants from National Basic Research Program of China (#2005CB522502 to A.M.M.), from Major Science Programs of China (#2006CB943401 to A.M.M.), from National Natural Science Foundation of China (#90208002 and #30221003 to A.M.M.), from TRAPOYT of the MOE (to A.M.M.), from the Centre National de la Recherche Scientifique, the Asssociation pour la Recherche contre le Cancer, the Ligue Nationale Contre le Cancer, the Ministère de la Recherche and from the National Institute of Health. F.-I.L. was supported by fund from the EU 6th Framework program (MYORES).

References

Bratt, A., Wilson, W. J., Troyanovsky, B., Aase, K., Kessler, R., Van Meir, E. G. and Holmgren, L. (2002). Angiomotin belongs to a novel protein family with conserved coiled-coil and PDZ binding domains. *Gene* **298**, 69-77.

Bratt, A., Birot, O., Sinha, I., Veitonmaki, N., Aase, K., Ernkvist, M. and Holmgren, L. (2005). Angiomotin regulates endothelial cell-cell junctions and cell motility. *J. Biol. Chem.* **280**, 34859-34869.

Bruckner, K., Pablo Labrador, J., Scheiffele, P., Herb, A., Seeburg, P. H. and Klein, R. (1999). EphrinB ligands recruit GRIP family PDZ adaptor proteins into raft membrane microdomains. *Neuron* **22**, 511-524.

Ciruna, B. and Rossant, J. (2001). FGF signaling regulates mesoderm cell fate specification and morphogenetic movement at the primitive streak. *Dev. Cell* **1**, 37-49.

Dupe, V., Ghyselinck, N. B., Thomazy, V., Nagy, L., Davies, P. J., Chambon, P. and Mark, M. (1999). Essential roles of retinoic acid signaling in interdigital apoptosis and control of BMP-7 expression in mouse autopods. *Dev. Biol.* **208**, 30-43.

Fincham, V. J., Unlu, M., Brunton, V. G., Pitts, J. D., Wyke, J. A. and Frame, M. C. (1996). Translocation of Src kinase to the cell periphery is mediated by the actin cytoskeleton under the control of the Rho family of small G proteins. *J. Cell Biol.* **135**, 1551-1564.

Frame, M. C. (2004). Newest findings on the oldest oncogene; how activated src does it. *J. Cell Sci.* **117**, 989-998.

Funke, L., Dakoji, S. and Bredt, D. S. (2005). Membrane-associated guanylate kinases regulate adhesion and plasticity at cell junctions. *Annu. Rev. Biochem.* **74**, 219-245.

Holmgren, L., Ambrosino, E., Birot, O., Tullus, C., Veitonmaki, N., Levchenko, T., Carlson, L. M., Musiani, P., Iezzi, M., Curcio, C. et al. (2006). A DNA vaccine targeting angiomotin inhibits angiogenesis and suppresses tumor growth. *Proc. Natl. Acad. Sci. USA* **103**, 9208-9213.

Huttelmaier, S., Zenklusen, D., Lederer, M., Dictenberg, J., Lorenz, M., Meng, X., Bassell, G. J., Condeelis, J. and Singer, R. H. (2005). Spatial regulation of beta-actin translation by Src-dependent phosphorylation of ZBP1. *Nature* **438**, 512-515.

Ip, Y. T. and Gridley, T. (2002). Cell movements during gastrulation: snail dependent and independent pathways. *Curr. Opin. Genet. Dev.* **12**, 423-429.

Ishizawar, R. and Parsons, S. J. (2004). c-Src and cooperating partners in human cancer. *Cancer Cell* **6**, 209-214.

Jiang, W. G., Watkins, G., Douglas-Jones, A., Holmgren, L. and Mansel, R. E. (2006). Angiomotin and angiomotin like proteins, their expression and correlation with angiogenesis and clinical outcome in human breast cancer. *BMC Cancer* **6**, 16.

Jopling, C. and den Hertog, J. (2005). Fyn/Yes and non-canonical Wnt signalling converge on RhoA in vertebrate gastrulation cell movements. *EMBO Rep.* **6**, 426-431.

Kaplan, K. B., Swedlow, J. R., Varmus, H. E. and Morgan, D. O. (1992). Association of p60c-src with endosomal membranes in mammalian fibroblasts. *J. Cell Biol.* **118**, 321-333.

Levchenko, T., Aase, K., Troyanovsky, B., Bratt, A. and Holmgren, L. (2003). Loss of responsiveness to chemotactic factors by deletion of the C-terminal protein interaction site of angiomotin. *J. Cell Sci.* **116**, 3803-3810.

Levchenko, T., Bratt, A., Arbiser, J. L. and Holmgren, L. (2004). Angiomotin expression promotes hemangioendothelioma invasion. *Oncogene* **23**, 1469-1473.

Lo, J., Lee, S., Xu, M., Liu, F., Ruan, H., Eun, A., He, Y., Ma, W., Wang, W., Wen, Z. et al. (2003). 15000 unique zebrafish EST clusters and their future use in microarray for profiling gene expression patterns during embryogenesis. *Genome Res.* **13**, 455-466.

Marlow, F., Topczewski, J., Sepich, D. and Solnica-Krezel, L. (2002). Zebrafish Rho kinase 2 acts downstream of Wnt11 to mediate cell polarity and effective convergence and extension movements. *Curr. Biol.* **12**, 876-884.

Myers, D. C., Sepich, D. S. and Solnica-Krezel, L. (2002). Bmp activity gradient regulates convergent extension during zebrafish gastrulation. *Dev. Biol.* **243**, 81-98.

Nelson, W. J. and Nusse, R. (2004). Convergence of Wnt, beta-catenin, and cadherin pathways. *Science* **303**, 1483-1487.

Nourry, C., Grant, S. G. and Borg, J. P. (2003). PDZ domain proteins: plug and play! *Sci. STKE* **2003**, RE7.

Nutt, S. L., Dingwell, K. S., Holt, C. E. and Amaya, E. (2001). Xenopus Sprouty2 inhibits FGF-mediated gastrulation movements but does not affect mesoderm induction and patterning. *Genes Dev.* **15**, 1152-1166.

Sandilands, E., Cans, C., Fincham, V. J., Brunton, V. G., Mellor, H., Prendergast, G. C., Norman, J. C., Superti-Furga, G. and Frame, M. C. (2004). RhoB and actin polymerization coordinate Src activation with endosome-mediated delivery to the membrane. *Dev. Cell* **7**, 855-869.

Schier, A. F. and Talbot, W. S. (2005). Molecular genetics of axis formation in zebrafish. *Annu. Rev. Genet.* **39**, 561-613.

Shimono, A. and Behringer, R. R. (2003). Angiomotin regulates visceral endoderm movements during mouse embryogenesis. *Curr. Biol.* **13**, 613-617.

Solnica-Krezel, L. (2005). Conserved patterns of cell movements during vertebrate gastrulation. *Curr. Biol.* **15**, R213-R228.

Thisse, B. and Thisse, C. (2005). Functions and regulations of fibroblast growth factor signaling during embryonic development. *Dev. Biol.* **287**, 390-402.

Thisse, B., Heyer, V., Lux, A., Alunni, V., Degrave, A., Seiliez, I., Kirchner, J., Parkhill, J. P. and Thisse, C. (2004). Spatial and temporal expression of the zebrafish genome by large-scale in situ hybridization screening. *Methods Cell Biol.* **77**, 505-519.

Thomas, S. M. and Brugge, J. S. (1997). Cellular functions regulated by Src family kinases. *Annu. Rev. Cell Dev. Biol.* **13**, 513-609.

Tian, T. and Meng, A. M. (2006). Nodal signals pattern vertebrate embryos. *Cell. Mol. Life Sci.* **63**, 672-685.

Timpson, P., Jones, G. E., Frame, M. C. and Brunton, V. G. (2001). Coordination of cell polarization and migration by the Rho family GTPases requires Src tyrosine kinase activity. *Curr. Biol.* **11**, 1836-1846.

Topczewski, J., Sepich, D. S., Myers, D. C., Walker, C., Amores, A., Lele, Z., Hammerschmidt, M., Postlethwait, J. and Solnica-Krezel, L. (2001). The zebrafish glypican knypek controls cell polarity during gastrulation movements of convergent extension. *Dev. Cell* **1**, 251-264.

Troyanovsky, B., Levchenko, T., Mansson, G., Matvijenko, O. and Holmgren, L. (2001). Angiomotin: an angiostatin binding protein that regulates endothelial cell migration and tube formation. *J. Cell Biol.* **152**, 1247-1254.

Warga, R. M. and Kimmel, C. B. (1990). Cell movements during epiboly and gastrulation in zebrafish. *Development* **108**, 569-580.

Wells, C. D., Fawcett, J. P., Traweger, A., Yamanaka, Y., Goudreault, M., Elder, K., Kulkarni, S., Gish, G., Virag, C., Lim, C. et al. (2006). A Rich1/Amot complex regulates the Cdc42 GTPase and apical-polarity proteins in epithelial cells. *Cell* **125**, 535-548.

Xiong, B., Rui, Y., Zhang, M., Shi, K., Jia, S., Tian, T., Yin, K., Huang, H., Lin, S., Zhao, X. et al. (2006). Tob1 controls dorsal development of zebrafish embryos by antagonizing maternal beta-catenin transcriptional activity. *Dev. Cell* **11**, 225-238.

Yang, X., Dormann, D., Munsterberg, A. E. and Weijer, C. J. (2002). Cell movement patterns during gastrulation in the chick are controlled by positive and negative chemotaxis mediated by FGF4 and FGF8. *Dev. Cell* **3**, 425-437.

Zhang, L., Zhou, H., Su, Y., Sun, Z., Zhang, H., Zhang, L., Zhang, Y., Ning, Y., Chen, Y. G. and Meng, A. (2004). Zebrafish Dpr2 inhibits mesoderm induction by promoting degradation of nodal receptors. *Science* **306**, 114-117.

Zhao, J., Cao, Y., Zhao, C., Postlethwait, J. and Meng, A. (2003). An SP1-like transcription factor Spr2 acts downstream of Fgf signaling to mediate mesoderm induction. *EMBO J.* **22**, 6078-6088.